Numerical Modeling for Supersonic Flow Analysis and Inverse Design

K. Matsushima.* D. Maruyama† and T. Matsuzawa‡
Department of Aerospace Engineering, Tohoku University, Sendai, Japan, 980-8579

For the aerodynamic wing design, the superior points of a inverse problem method are discussed as well as two mathematical models each of which is the core equation of each inverse problem are introduces. One mathematical model comes from three-dimensional potential flow equation and he thin wing theory, while the other is led from Busemann's 2nd order approximation based on the theory of oblique shock wave. The former yields the set of integral-differential equations and the latter does a quadratic equation in the corresponding inverse problem. Combining each inverse problem with residual-correction methodology and modern computational technology enables us to construct a low-cost and high-fidelity design method. To examine its capability and usefulness, several design problems have been done. Successful high-fidelity design results have been obtained for all cases. The computational cost is small. The inverse design needs about 20 time flow simulations which is much less than the cost of a general optimization.

Nomenclature

a	=	speed of sound
a_∞	=	free-stream speed of sound
C_p	=	pressure coefficient
ΔC_p	=	difference between realized pressure coefficient and target one
c	=	chord length of an airfoil
c_1, c_2	=	Busemann coefficients
$f(x)$, $f(x,y)$	=	wing section/ airfoil geometry
Δf	=	amount of correction/ modification in wing section/ airfoil geometry
M_∞	=	free-stream Mach number
P	=	pressure
P_∞	=	free-stream pressure
Re	=	Reynolds number
t	=	airfoil thickness
x	=	airfoil-chord direction coordinate
y	=	span-wise direction coordinate
z	=	airfoil-thickness direction coordinate
α	=	angle of attack
β	=	$\sqrt{M_\infty^2 - 1}$
γ	=	ratio of specific heats
ρ	=	density
ρ_∞	=	free-stream density
ϕ	=	velocity potential
θ	=	$df/dx - \alpha$ (flow deflection angle)

1 Introduction

Efficient design optimization methods are still sought after for use in aerodynamic design, though the computer performance and computational fluid dynamic (CFD) simulation technology have made great progress in these several decades. Therefore, engineers have become to desire higher-fidelity design as they have obtained more advanced simulation tools. Conventional design methods, such as gradient based one and Genetic algorithm (GA), perform optimizations using direct CFD computations. CFD computations sometimes mean Euler ones and sometimes Navier-Stokes (N-S). They, especially N-S computations still take much time to get results in sufficient detail. Usually the optimizations need a lot of number of CFD computations. Thus, the

* Associate Professor, Department of Aerospace Engineering, Email :kisam@ad.mech.tohoku.ac.jp
† Graduate Research assistant, Department of Aerospace Engineering,
‡ Graduate student, Department of Aerospace Engineering,

resulting process can be computationally very expensive. Then, designers have to limit design space or reduce the number of design parameters to save the computational cost. In this situation, could we regard the design as high-fidelity design? Flow analysis is of high fidelity, if N-S simulation with sufficient grid resolution is conducted. But, the design is not necessarily of high fidelity because they might examine only a small part of whole possible candidates.

There is another design methodology called as inverse design or (inverse problem methods). Inverse design determines the values of a set of design parameters by matching special target flow features given by a designer. They usually use mathematical models to find the solution for the set of design parameters that result in the target flow features. Inverse designs have proven valuable because once a solvable target flow feature is specified the required geometry can be obtained with fewer CFD valuations compared to a direct optimization. The refined knowledge of the target flow features allows rapid convergence towards the final design. Particularly, in the context of aerodynamic wing design, the flow feature should be surface Cp distribution. So the inverse problem provides wing geometry which realizes the target Cp distribution.

Classical inverse problem method was categorized as a low-fidelity design, since the method used mathematical models, which had been led from low-fidelity equations such as potential equation, linearized one and so on. With modern CFD technology, however, the method has attained high-fidelity design by combined with residual-correction methodology. We will discuss the methodology in Section 2. There, low-cost high-fidelity design method using inverse design and CFD computation is constructed. In Section 3, a mathematical model for three-dimensional supersonic flowfields will be discussed. An inverse design method using the model was already applied to a practical supersonic wing design [1,2] in JAXA's NEXST project [3,4]. The successful design results have been confirmed by the flight test on October 10 in 2005 [5,6]. In Section 4, another mathematical model will be discussed. The model originated from A. Busemann[7,8]. It was led by higher order approximation than the first one but is two- dimensional. The second one is being applied to the design of practical airfoils /wing-sections in a complicated flowfield. Its design applications will be also presented in the next paper. In Section 5, we will conclude the article.

At the end of the introduction, we mention additional favorable characteristic about the inverse design. In the design we can trace precise geometrical change of the wing surface because the number of geometrical control points used for the design is not strictly limited. In the case of setting 100 points in the chord direction on each of 100 span stations of the wing, which means the number of control points on the wing geometry is totally 10,000, the cost of solving a inverse problem is about 10 minutes with a 2.2Ghz PC.

2 Residual-Correction Methodology for Aerodynamic Inverse Design

The goal of the aerodynamic inverse design is to determine the surface geometry which realizes a specified target pressure distribution. The procedure is iterative. It can design a wing for not only a wing alone case but also any types of aircraft configuration.

Here the task sequence of a residual-correction method is illustrated. First, a baseline shape is to be defined. If one would like to design a wing for an airplane, the initial/ baseline shape is not a wing alone but a complete airplane where a wing is jointed with a fuselage. Then, the flowfield around a airplane is analyzed by CFD simulation to get the current pressure (Cp) distribution on the wing surface. Next the inverse problem is solved to obtain the geometrical correction value Δf corresponding to the difference between target and current pressure distributions ΔCp. Using Δf, the baseline shape is modified to be a new wing. Now, the current shape is updated. The next step is to go back to the flowfield analysis. The flow analysis is again conducted to see if the current shape realizes target pressure distribution. If the difference between target and current pressure distributions is negligible, the design is completed. Otherwise, the next step is once again to solve the inverse problem and iterate the design loop until the pressure difference becomes negligible. This iterative procedure of residual-correction concept expands the applicability of the inverse problem. Classically, the fidelity of the solution to an inverse problem method is within the extent of the basic equation to formulate the inverse problem. On the other hand, the solution can attain higher fidelity when the inverse problem is appropriately incorporated into a residual-correction method.

There are two primary parts in the design system; one is a flow analysis part which conducts grid generation and Navier-Stokes/Euler flow simulation. It evaluates the residual. The other is a design part where the inverse problem is solved to update the geometry. The design part determines the correction which is expected to compensate for the residual. Both parts are independent from each other in terms of their algorithms and basic equations as long as they are originated from flow physics. The accuracy of a design result depends on the analysis part. The flow analysis is done by a Navier-Stokes simulation code. Thus, designed geometry

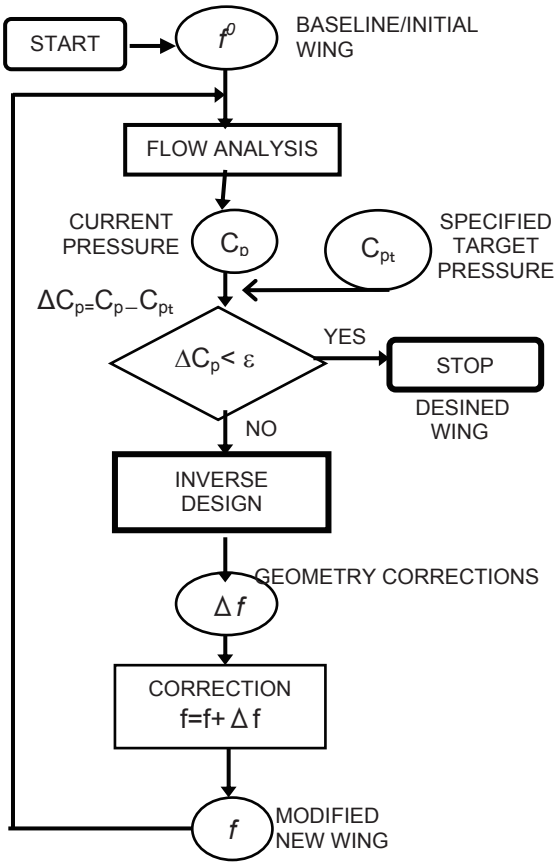

Figure 1. Residual-correction design concept

by the method will have the same fidelity as Navier-Stokes equations do.

3 An Supersonic Inverse Problem based on Three Dimensional Thin Wing Theory

3.1 Formulation of an Inverse Problem and Derived Mathematical Models

The basic equations of the first inverse problem that determines the aerodynamic geometry are

$$\left(1-M_{\infty}^{2}\right)\overline{\phi}_{\overline{x}\overline{x}}+\overline{\phi}_{\overline{y}\overline{y}}+\overline{\phi}_{\overline{z}\overline{z}}=0 \tag{3-1}$$

$$\overline{\phi}_{\overline{z}}\left(\overline{x},\overline{y},\pm 0\right)=\frac{\partial}{\partial\overline{x}}f_{\pm}\left(\overline{x},\overline{y}\right) \tag{3-2}$$

$$Cp_{\pm}\left(\overline{x},\overline{y}\right)=-2\overline{\phi}_{\overline{x}}\left(\overline{x},\overline{y},\pm 0\right) \tag{3-3}$$

where "¯" (over bar) indicates that values and functions are in the physical coordinate which has dimension.

Eq.(3-1) is the small disturbance velocity potential equation. Since M_{∞}>1.0 in supersonic flows, Eq.(3-1) is hyperbolic partial differential equation (PDE). Eq.(3-2) comes from thin wing theory and Eq.(3-3) is led by linearizng the Bernoulli equation in compressible flows [9]. The goal of the formulation is to obtain the mathematical function to relate ΔCp to geometrical correction of wing surface Δf. As stated in the previous section, the inverse problem of the residual-correction concept should handle the Δ-value, which is difference between two states of a flowfield. Thus, we take linear perturbation form of Eqs. (3-1) to (3-3) after the Prandtl-Glauert transformation Then, applying Green's theorem to the hyperbolic PDE and performing calculus on the resulted equation, we finally obtain following equations.

$$\Delta w_s(x,y)=-\Delta u_s(x,y)-\frac{1}{\pi}\iint_{\tau_+}\frac{(x-\xi)\Delta w_s(\xi,\eta)}{[(x-\xi)^2-(y-\eta)^2]^{3/2}}\,d\eta d\xi \tag{3-4}$$

$$where\quad \Delta u_s(x,y)=-\frac{1}{2\beta^2}(\Delta Cp_+ + \Delta Cp_-) \tag{3-5}$$

$$\Delta w_s(x,y)=\frac{1}{\beta^3}\frac{\partial}{\partial x}(\Delta f_+ - \Delta f_-) \tag{3-6}$$

$$\Delta w_a(x,y)=-\Delta u_a(x,y)-\frac{1}{\pi}\iint_{\tau_+}\frac{(x-\xi)\Delta u_a(\xi,\eta)}{(y-\eta)^2\sqrt{(x-\xi)^2-(y-\eta)^2}}\,d\eta d\xi \tag{3-7}$$

$$where\quad \Delta u_a(x,y)=-\frac{1}{2\beta^2}(\Delta Cp_+ - \Delta Cp_-) \tag{3-8}$$

$$\Delta w_a(x,y)=\frac{1}{\beta^3}\frac{\partial}{\partial x}(\Delta f_+ + \Delta f_-) \tag{3-9}$$

Equations. (3-4) and (3-7) are the mathematical models to relate pressure differences to geometrical correction. The x coordinate is chord-wise and the y coordinate is span-wise. It is illustrated in Fig. 2. In Eqs. (3-4) and (3-7), ξ and η are integral variables which correspond to x and y, respectively. The z coordinate is in the wing thickness direction. The models reduce three-dimensional problem to two-dimensional surface integrals. The subscript + indicates that the variable is on the upper surface of the wing while the subscript – indicates the lower surface. The area for integration, denoted by τ+, is the upper wing surface limited by the forwarded Mach cone from a point P(x,y) and leading edge line. The $y=\eta$ line (the singular cylinder in Fig. 2) is excluded from the integration area τ+. The Mach cone, P and τ+ are also shown in Fig. 2.

For design we use the models to determine the geometrical correction; Δw is unknown; Δu is given. Eq. (3-4) is a Volterra integral equation of the second kind for Δw_s. Δw_s is associated with the chord-wise thickness change at (x, y) on a wing. Eq. (3-7) is the integral expression for Δw_a, which is associated with the chord-wise curvature change of the wing section camber, at (x, y). The geometrical correction function, Δf, which is the z coordinate modification of the wing surface, is calculated using $\Delta w_s(x,y)$ and $\Delta w_a(x,y)$;

$$\Delta f_{\pm}(x,y/\beta)=\frac{1}{2\beta^3}\int_{L.E.}^{x}[\Delta w_s(\xi,y)\pm\Delta w_a(\xi,y)]d\xi \tag{3-10}$$

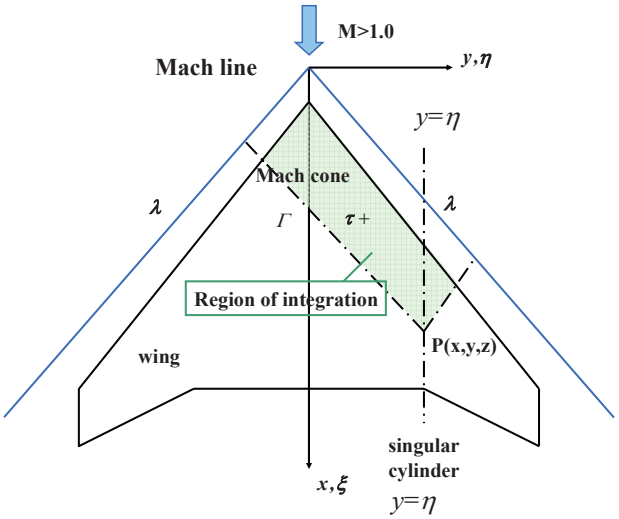

Figure 2 Flowfield and coordinate system for formulation.

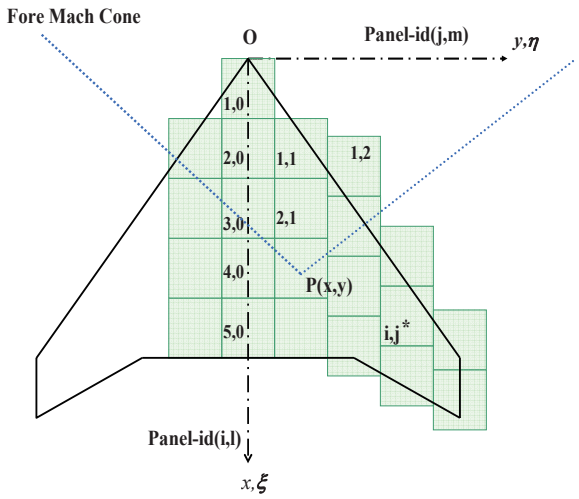

Figure 3 Panels on wing surface.

Discretization

To solve those integral equations presented in the previous subsection computationally, the wing surface is discretized into small rectangular panels as shown in Fig. 3. Then the double integrals of Eqs.(3-4) and (3-7) become the summation of piecewise integrals inside each panel. The piecewise integrals are evaluated at the center of each panel which is indicated as P(*i, j*) in Fig. 3. This lets us avoid the leading edge singularity. By assuming Δu_s, Δu_a, Δw_s and Δw_a to be constant inside a panel, piecewise integrals can be analytically calculated.

3.2 Application to Japanese SST Project Wing design [1,2]

The wing of a scaled experimental SST called NEXST-1 was designed by the inverse problem with the residual-correction method. They aimed to naturally realize wide laminar flow area on the main wing. Figure 4 shows the outlook of NEXST-1 and the main wing. The design was successfully performed. In Oct. 10, 2005 a flight test succeeded and they obtained fruitful test results. Finally the results confirmed the reliability of the inverse design.

The design was done at M_∞=2.0. In order to realize a wide natural laminar flow region on the wing, the special target Cp distributions were prescribed (see Fig. 7). The inverse design to determine geometry, we used 50 (chord-wise)×82 (span-wise) panels on the half span of a wing and solved the inverse problem with the target Cp. For analytical part, Navier-Stokes simulations were conducted. JAXA's UPACKS code [10] was used to obtain current surface Cp distributions over the wing.

The design results are shown in Figs. 6 and 7. Figure 6 compares the realized Cps of a designed wing with those of the baseline and the target Cps. They are the surface Cp distributions around the wing section at the 50% semi span-station. It is clearly seen that the realized Cps agrees with the target much better than the baseline does. On the upper surface and around leading edge, both of the realized and target Cps are identical. Figure 7 is the comparison of wing sections geometry of the baseline and designed wing. The new type of section airfoil geometry beyond traditional knowledge and experience was theoretically obtained by the numerical inverse design using the mathematical model.

3.3 Other Application of the Mathematical Models

The derived mathematical models in Section 3.1, which are Eqs.(3-4) and (3-7), can be applied to more complicated designs [11,12] and other analysis. In addition, they can be used to solve direct problems. If geometry, Δw_s and Δw_a is given, the surface Cps, Δu_s and Δu_a are simply calculated. The calculated Cps are accurate in potential flow estimation level, but the cost is surprisingly low. The useful application may be that to aerodynamic interaction among multi bodies in a flowfield [11].

The models can also be used to analyze aerodynamic effect of geometry on surface Cp distribution. For example, we can segregate two-dimensional effect from three-dimensional one and then compare the influential coefficient on the Cp value at the point P. Simply speaking, the integral part of each equation indicates the three-dimensional effect and the rest does two-dimensional one.

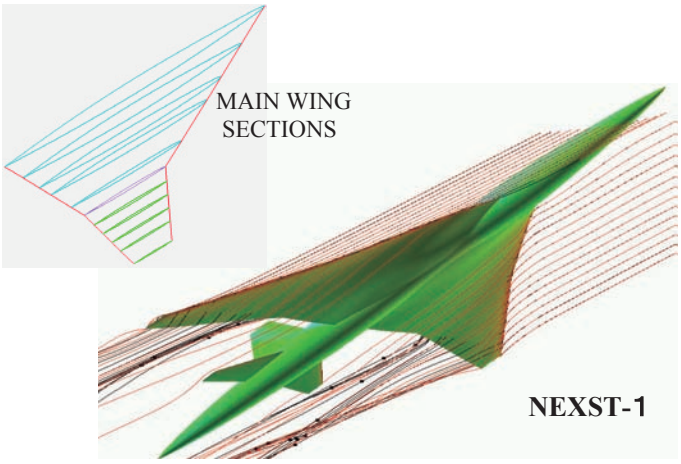

Figure 5 Flowfield around NEXST-1 and wing sections at span-stations of the main wing.

Figure 6 NEXST-1 flight test. (Ref. 4)

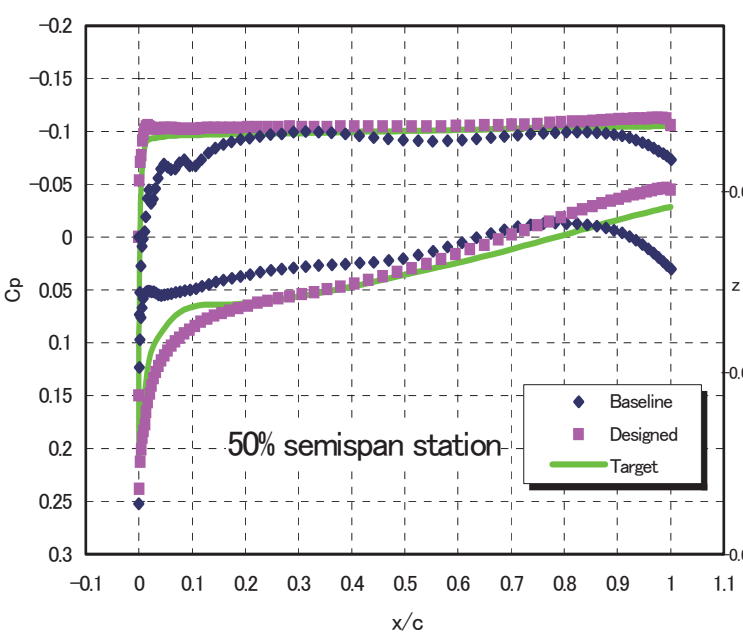

Figure 7 Design results; comparison of surface Cp distributions by computation.

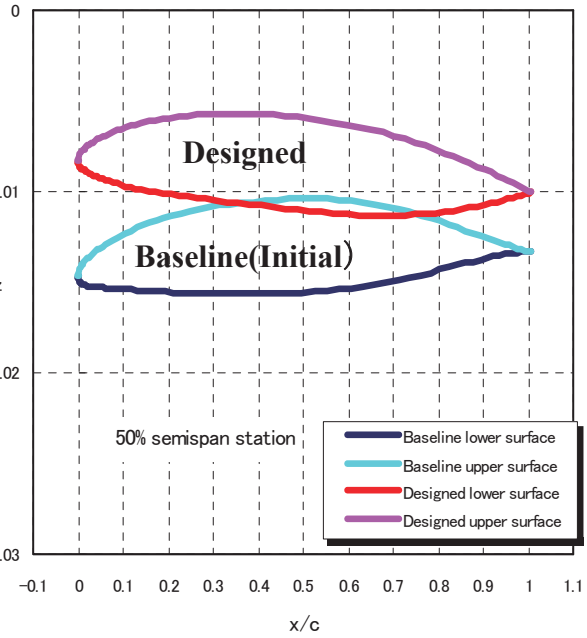

Figure 8 Design results; comparison of a wing section geometry.

4 An Inverse Problem based on Oblique Shock Relation

4.1 Formulation of an Inverse Problem and Derived Mathematical Models

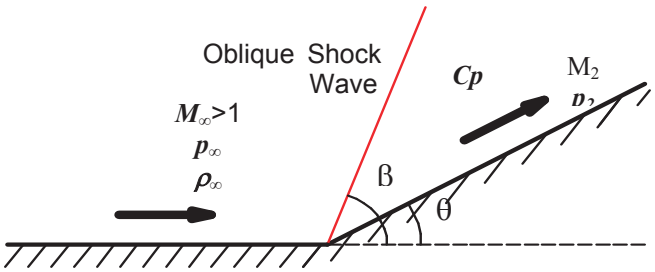

Figure 9 Super sonic flow along a compression corner.

In this formulation, we assume a small flow deflection angle θ is related to Cp values downstream of oblique shock waves by the following local oblique shock relations;

$$Cp = \frac{p_2 - p_\infty}{\frac{1}{2}\rho_\infty M_\infty^2 a_\infty^2} = \frac{4}{(\gamma+1)M_\infty^2}(M_\infty^2 \sin^2\beta - 1) \qquad (4\text{-}1)$$

$$M_\infty^2 \sin^2\beta - 1 = \frac{\gamma+1}{2} M_\infty^2 \frac{\sin\beta \sin\theta}{\cos(\beta-\theta)} \qquad (4\text{-}2)$$

and the asymptotic expansion of $\tan\beta$ when $\sin\mu$ is M_∞^{-1}; β is the oblique shock wave angle to the un-deflected flow direction.

$$\tan\beta = \tan(\mu + \varepsilon) = \tan\mu + \frac{1}{\cos^2\mu}\varepsilon + \frac{\sin\mu}{\cos^3\mu}\varepsilon^2 \qquad (4\text{-}3)$$

Manipulating Eqs. (4-1) to (4-3) and neglecting the more than third order terms of θ, we obtain

$$Cp = c_1\theta + c_2\theta^2 \quad \text{where} \quad c_1 = \frac{2}{\sqrt{M_\infty^2 - 1}}, \quad c_2 = \frac{(M_\infty^2 - 2)^2 + \gamma M_\infty^4}{2(M_\infty^2 - 1)^2} \qquad (4\text{-}4)$$

c_1 and c_2 are Busemann's coefficient[8]. Equation (4-4) holds both of compression and expansion corner. For compression, the flow deflection angle θ is positive, while the angle θ is negative for expansion. This relation is applied to the upper and lower surface of an airfoil. Then we have following equations.

$$Cp_+ = c_1\left(\frac{df_+(x)}{dx} - \alpha\right) + c_2\left(\frac{df_+(x)}{dx} - \alpha\right)^2 \qquad (4\text{-}5)$$

$$Cp_- = -c_1\left(\frac{df_-(x)}{dx} - \alpha\right) + c_2\left(\frac{df_-(x)}{dx} - \alpha\right)^2 \qquad (4\text{-}6)$$

α is the angle of attack of the airfoil. x represents the airfoil-chord direction (see Fig. 10). Subscripts + and – denote the upper and lower surfaces respectively.

Equations (4-5) and (4-6) may be used for design problems. In Ref.13, an SST wing design was performed using the both equations. Here, we adopt the perturbation form (Δ-form) of the equations As demonstrated in Section 2, a design method using a perturbation form extends the applicability of the. Therefore, taking the small perturbation ($C_p \rightarrow C_p + \Delta C_p$ and $f \rightarrow f + \Delta f$) of Eqs.

(4-5) and (4-6), we obtain Δ-form equations. An inverse-problem solves the *x*-derivative of the correction value for the airfoil geometry, $d\Delta f_{\pm}/dx$; this *x*-derivative is related to the difference between the target and the current pressure distributions, denoted as ΔC_p (C_p-residual). Specifically, the geometry correction term Δf (see Fig. 4) comes from ΔC_p, using the small-perturbation forms ($C_p \to C_p + \Delta C_p$ and $f \to f + \Delta f$) of Eq. (4).

$$\Delta Cp_{+} = c_1\left(\frac{d\Delta f_{+}(x)}{dx}\right) + 2c_2\left(\frac{d f_{+}(x)}{dx} - \alpha\right)\left(\frac{d\Delta f_{+}(x)}{dx}\right) + c_2\left(\frac{d\Delta f_{+}(x)}{dx}\right)^2 \tag{4-7}$$

$$\Delta Cp_{-} = -c_1\left(\frac{\mathrm{d}\Delta f_{-}(x)}{\mathrm{d}x}\right) + 2c_2\left(\frac{\mathrm{d} f_{-}(x)}{\mathrm{d}x} - \alpha\right)\left(\frac{\mathrm{d}\Delta f_{-}(x)}{\mathrm{d}x}\right) + c_2\left(\frac{\mathrm{d}\Delta f_{+}(x)}{\mathrm{d}x}\right)^2 \tag{4-8}$$

The airfoil geometry is updated by integrating the geometry correction terms:

$$f_{\pm}^{update}(x) = f_{\pm}(x) + \int_0^x \frac{\mathrm{d}\,\Delta f_{\pm}}{\mathrm{d}\,\xi}(\xi)\,\mathrm{d}\xi \tag{4-9}$$

where the symbol 0 indicates the x coordinate of the airfoil's leading edge. Finally, we have another mathematical model to relate pressure change to airfoil's geometry modification [14].

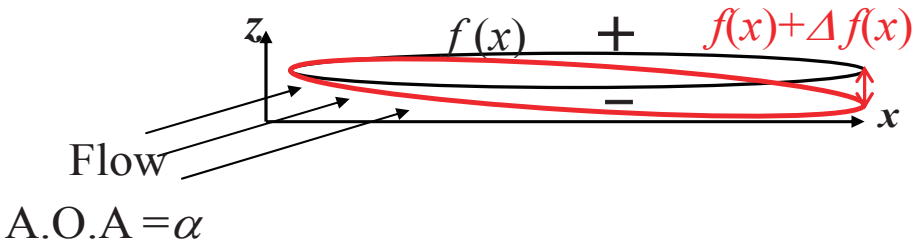

Figure 10. Airfoil geometries based on the current and target pressure distributions.

4.2 Application – Aerodynamic Design of Biplane Airfoils –

The above-mentioned inverse problem design method has been validated. To check its applicability we conducted an airfoil design in a complicated flowfield. The design object is a biplane, where two airfoils strongly interact with each other. Figure 11 is the initial/baseline configuration. We attempted to design the upper element of the biplane by specifying the obtained C_p distribution of an existing biplane by the computation. The design target was a known airfoil, that was the Busemann biplane [15]shown in Fig. 12. During the design process, the shape of the lower element of the biplane remained fixed (see Figs. 11 and 12). This was two dimensional design so the wing of infinite span length was assumed. The design was for the biplane flying at M_∞ = 1.7. In this design, Euler flow simulations were conducted using Tohoku University Aerodynamic Simulation (TAS) code [16]. All the simulations used the same size grid distribution to avoid counting uncertainty error due to the grid size effect during the design process. Through the design, it has been confirmed that the upper element which starts from an arbitrary airfoil geometry converges to the target geometry.

As seen in Fig, 13-(a), the initial geometry of the upper element was a thin flat plate. Figure 13-(b) shows the initial Cp distributions around both of upper and lower airfoils. The target geometry is presented in Fig. 14 with the design result. The pressure distributions around the Busemann biplane (Fig. 12) obtained by analyzing at Mach 1.7 speed are adopted as the target C_p. It is shown in Fig. 15. After 14 times iterations, the realized C_p distribution by the designed airfoil has converged to the target one. In Figs. 14 and 15 the designed geometry and resulted Cp distributions are also presented. Both of geometry and Cp distributions of designed airfoil are identical to those of the target one. Actually, the absolute Root Mean Square (RMS) error between the realized C_p distribution and the target one is 1.4E-4.So the design has been successfully done [17].

The history of the design process is shown in Fig. 16. There, current results from the initial to the 3rd iteration are sequentially displayed. Current airfoil geometry and C_p distribution are presented compared with the target ones. In early stage of the design process, the change in Cp distributions at the airfoil rear part is drastic because of interaction between two elements of the biplane. After the 3rd iteration, the amount of change became smaller as the number of iteration increased; in other words the design converged uniformly to the target geometry. After the 14th iteration, as discussed before and can be seen in Fig. 15 again, the realized C_p by the designed geometry converged to the target one. It has been confirmed that the design method is capable of

performing the aerodynamic design of not only single airfoils but also biplanes where two airfoil elements interfere with each other.

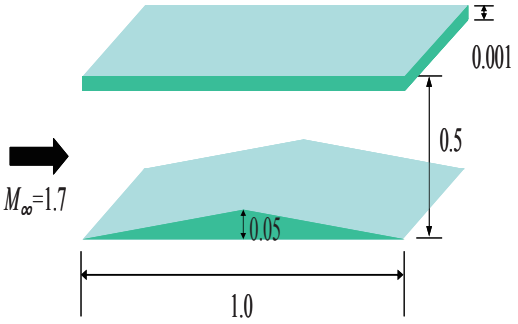

Figure 11 Initial geometry (M_∞=1.7).

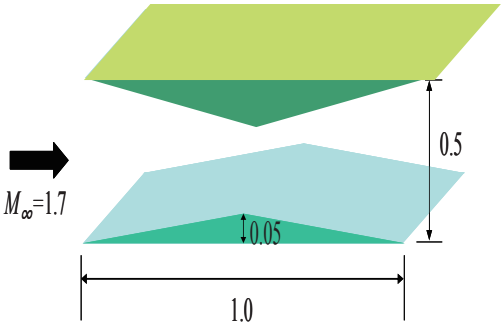

Figure 12 Target geometry (upper element) (M_∞=1.7).

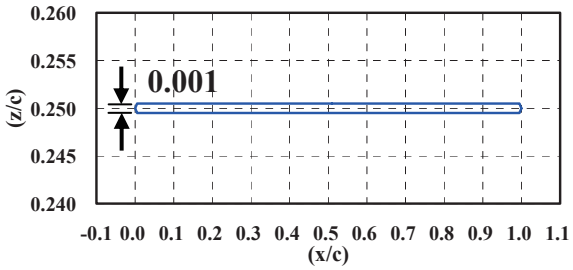

(a) Airfoil geometry of upper element

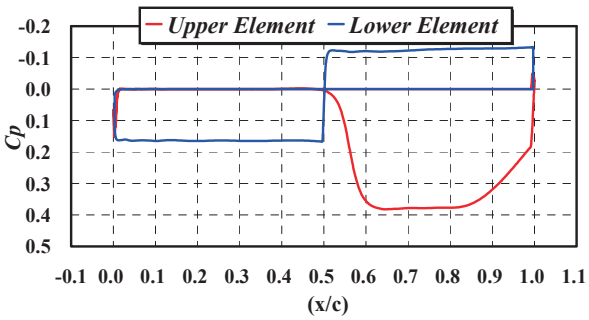

(b) *Cp* distributions

Figure 13 Section airfoil geometry and C_p distributions of initial geometry.

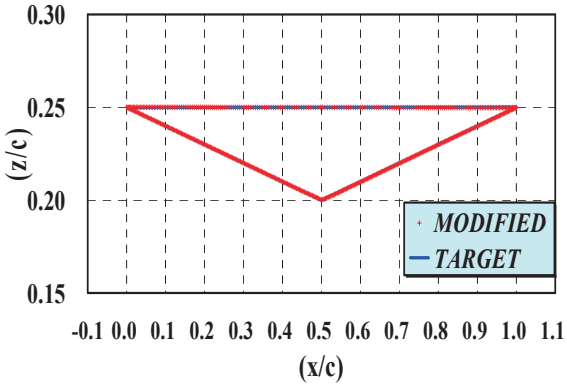

Figure 14 Designed geometry of the upper element.

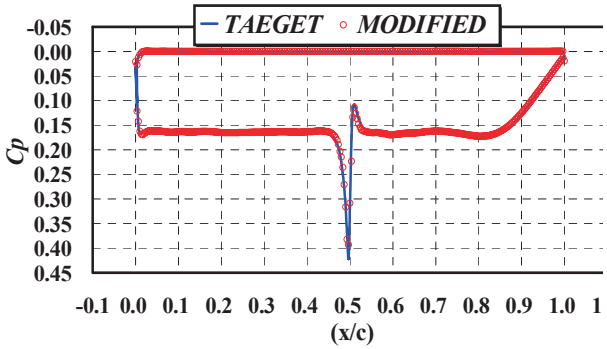

Figure 15 C_p distribution of upper element after 14 time iterations.

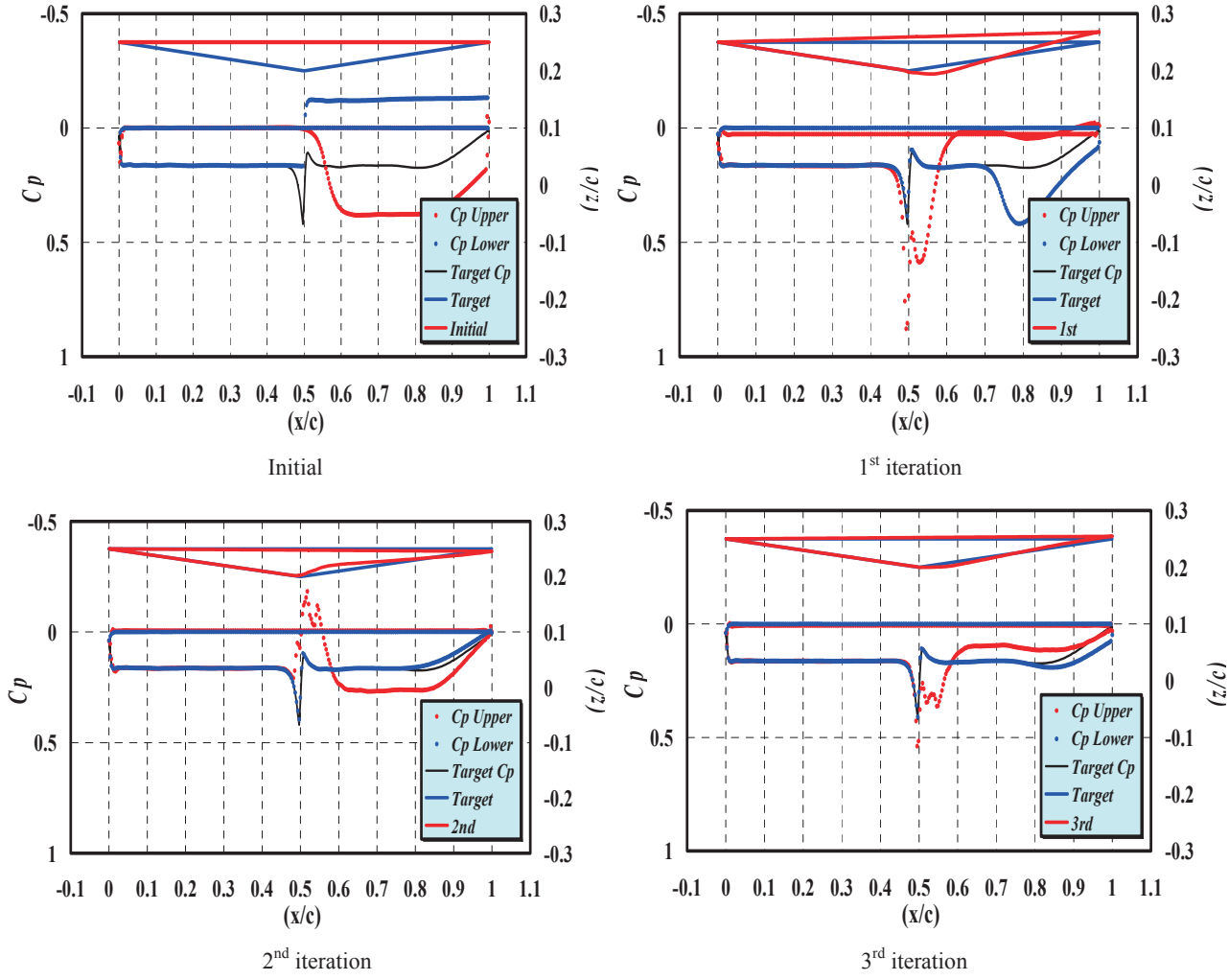

Figure 16 C_p distributions and geometries of modified airfoils during the early stage of design process.

5 Conclusions

For the aerodynamic wing design, the superior points of a inverse problem method are discussed as well as two mathematical models each of which is the core equation of an inverse problem are introduces. One mathematical model comes from three-dimensional potential flow equation and he thin wing theory, while the other is led from Busemann's 2nd order approximation based on the theory of oblique shock wave. The former yields the set of integral-differential equations and the latter does a quadratic equation in the corresponding inverse problem. Combining each inverse problem with residual-correction methodology and modern computational technology enables us to construct a low-cost and high-fidelity design method. To examine its capability and usefulness, several design problems have been done. For the first inverse problem, the design has been performed on a main wing for a scaled SST which realizes wide laminar region on its upper surface. This is a practical design problem in a real production. As for the other one, the biplane airfoil has been designed. The flowfield is complicated so, the design should be hard to converge because two airfoils of the biplane strongly interact with each other. Successful high-fidelity design results have been obtained for all cases. The computational cost is small. The inverse design needs about 20 time flow simulations which is much less than the cost of a general optimization. Consequently, the iterative inverse design methods have been proved efficient and accurate. We are now trying to utilize the mathematical models devised here for other flow analyses.

We would like to conclude this article with an additional advantage of inverse methods. It was indicated in a paper [18] by a famous experienced designer of the Boeing company. The paper stated that an inverse method to use computer could be a new way to revolutionize the design process because it would be not a copy or extension of traditional thought, but complements to human imagination.

References

[1] Matsushima, K., Jeong, S., Takaki, R., Obayashi, S., Nakahashi, K. and Iwamiya, T., "A Supersonic Inverse Wing Design Method and Its Applicaion to Japanese SST," Lecture Note in Physics Vol. 515 Springer, 1998, pp. 79-84.

[2] Matsushima, K. Iwamiya, T., Ishikawa, H., "Supersonic Inverse Design of Wings for the Full Configuration of Japanese SST," ICAS 2000, Proceedings 22nd International Congress of Aeronautical Sciences, 2000 , pp. 213.1-213.8.

[3] Yoshida, K., Makino, Y., "Aerodynamic Design of Unmanned Scaled Supersonic Experimental Airplane in Japan", ECCOMAS 2004, Jyvaskyla, 2004, pp. 24-28.

[4] http://www.apg.jaxa.jp/res/stt/index.html and http://www.apg.jaxa.jp/res/stt/a03.html

[5] Ohnuki, T., Hirako, K., Sakata, K., "National Experimental Supersonic Transport Project," Proceedings of the 25th International Congress of the Aeronautical Sciences, 2006.

[6] Kwak, D., Yoshida, K., Ishikawa, H., Noguchi, M., "Flight Test Measurements of Surface Pressure on Unmanned Scaled Supersonic Experimental Airplane," AIAA Paper 2006-3483, June 2006

[7] Busemann, A., "Aerodynamic lift at supersonic speeds," Luftfahrtforschung, Ed.12, Nr.6, Oct.3, 1935, pp.210-220.

[8] Liepmann, H. W., and Roshko, A., *Elements of Gas Dynamics*, John Wiley & Sons, Inc., New York, 1957, p. 389.

[9] Heaslet, M. A. and Lomax, H.: Supersonic and Transonic Small Perturbation Theory, Vol. 6 of *High-Speed Aerodynamics and Jet Propulsion*, Princeton University Press, 1954, pp. 122-344.

[10] Japan Aerospace eXploration Agency (JAXA), Introduction to UPACS,

[11] Matsushima, K. Iwamiya, T., "An Improved Aerodynamic Inverse Design Method for Complex SST Configuration Combined with 3D NS Solver," Computational Fluid Dynamics 2000, Proceedings of the First International Conference on Computational Fluid Dynamics, ICCFD, 2001 , pp. 679-684.

[12] Matsuhima, K., Iwamiya, T., Nakahashi, K., "Wing design for supersonic transports using integral equation method," Engineering Analysis with Boundary Elements Vol.28, 2004, pp. 247-255.

[13] Ogoshi, H. and Shima E., "Role of CFD in Aeronautical Engineering (15)," Special Publication of National Aerospace Laboratory, SP-37, Proceedings of the 15th NAL Symposium, Tokyo, Japan, June 1997, pp.81-86.

[14] Matsushima, K., Maruyama, D., Nakano, T. and Nakahashi, K., "Aerodynamic Design of Low Boom and Low Drag Supersonic Transport using Favorable Wave Interference," Proceedings of The 36th JSASS Annual Meeting, Tokyo, Japan, April, 2005, pp. 130-133.

[15] Liepmann, H. W., and Roshko, A., *Elements of Gas Dynamics*, John Wiley & Sons, Inc., New York, 1957, pp. 107-123.

[16] Nakahashi, K., Ito, Y., and Togashi, F., "Some Challenge of Realistic Flow Simulations by Unstructured Grid CFD," International Journal for Numerical Methods in Fluids, Vol.43, 2003, pp.769-783.

[17] Maruyama, D., Matsushima, K., Kusunose, K., Nakahashi, K., "Aerodynamic Design of Biplane Airfoils for Low Wave Drag Supersonic Flight," AIAA paper 2006-3323, The 24th AIAA Applied Aerodynamics Conference, June 2006.

[18] McMasters, H. J., and Cummings, M. R.: Airplane Design---Past, Present, and Future, Journal of Aircraft, Vol. 39, No. 1 2002, pp. 10-17.